

Experiments on Quantum and Thermal Desorption from ^4He Films

D. L. Goodstein, R. Maboudian, F. Scaramuzzi,^(a) M. Sinvani,^(b) and G. Vidali^(c)

Low Temperature Physics, California Institute of Technology, Pasadena, California 91125

(Received 24 January 1985)

Desorption of He atoms from thin films may be resolved experimentally into quantum and thermal components. We show that quantum desorption becomes the dominant part of the signal in submonolayer films. We also show that, when all effects of collisions between desorbed atoms are eliminated, quantum desorption is not focused normal to the surface of optically polished sapphire crystals.

PACS numbers: 68.45.Da, 67.70.+n

The ability to investigate experimentally an instance in which a transition from condensed to gaseous states may be related directly to a single quantum event is of obvious importance. Some years ago, experiments were reported in which ballistic phonons in crystals¹ and ballistic phonons and rotons in liquid helium² gave rise, respectively, to desorption and evaporation of He atoms. More recently, both techniques have been refined to the point where they yielded convincing evidence of the existence of processes in which a single quasiparticle gave rise to a single desorbed³ or evaporated atom.⁴ In the context of desorption, this has been called the phonoatomic effect. The phonoatomic effect is of additional interest because it is potentially an effective spectrometer for high-frequency phonons, and can be a direct probe of microscopic processes at a crystal surface.

In this paper, we report experiments in which both the dependence of the phonoatomic effect on film thickness and the angular distribution of desorbed atoms are studied. Previously,¹ the phonoatomic effect has appeared as a distinct but small ($\sim 5\%$) contribution to the total desorption normal to the surface plane due to a high-temperature but low-intensity beam of phonons. By reducing the film thickness we are able, in the present work, to take advantage of thermal desorption kinetics⁵ to suppress thermal desorption and achieve signals which are dominated by the phonoatomic effect. We are also able, for the first time, to study the angular distribution of desorption under conditions in which the results cannot have been affected by collisions among the desorbing atoms, and in which thermal desorption may be separated experimentally from phonoatomic-effect desorption.

Assuming translational invariance of the surface leads to the expectation that at a plane surface, noninteracting atoms desorbed by single phonons with energies high compared to $k_B T_f$ (T_f is the temperature of the film) will be strongly concentrated in the direction perpendicular to the surface,^{6,7} and also that atoms desorbed at wider angles will have lower mean kinetic energies⁷ (the rainbow effect). These effects are a consequence of the condition that the interaction con-

serves both the phonon energy and the component of its momentum parallel to the surface. They are expected for phonoatomic, but not thermal desorption. Taborek⁷ has observed the predicted effects in atoms desorbed directly from the surface of a heater, but subsequent analysis has indicated that both the angular focusing and the rainbow effect observed were most probably consequences of collisions among desorbing atoms.⁸ Thus, the question of whether there is any kinematic focusing of desorbed atoms remains unresolved.

As a preliminary experiment, an apparatus similar to the one described in Ref. 3 was used. Basically, it consists of a fast heater (10-ns response time) evaporated on the bottom of a 1-cm-thick, optically polished sapphire crystal. The phonons travel ballistically through the crystal and cause He atoms to desorb from a hole in a mask placed on the upper surface. Three bolometers at angles $\Theta = 0^\circ$, $\sim 22^\circ$, and $\sim 45^\circ$ from the normal measure the time-of-flight (TOF) and angular distribution. The experimental geometry and a typical distribution are shown in Fig. 1. The first shoulder at

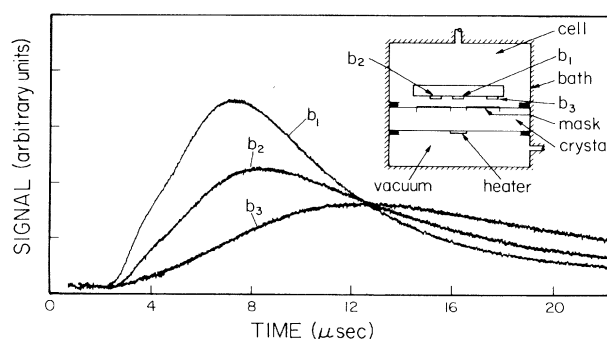


FIG. 1. Time-of-flight spectra at angles of approximately 0° , 22° , and 45° with respect to the surface normal (bolometers b_1 , b_2 , and b_3 , respectively). The inset shows the experimental geometry. The hole in the mask was 0.8 mm in diameter. The distance between the detector plane and the desorbing surface is 1.2 mm. The heater temperature was 19 K calculated according to acoustic mismatch. Ambient temperature was 2.4 K. A typical pulse width used was 180 ns. The chemical potential is roughly -30 K.

earlier times on curve b_1 represents atoms arriving with an associated temperature of about 9 ± 2 K. It is due to atoms desorbed by substrate phonons having an apparent temperature of 9 K. The second peak is due to the process in which phonons are thermalized, raising the temperature of the film slightly above the ambient (~ 2.4 K), and thus causing thermal desorption.

The absence of collisions in our experiment is a consequence of the low rate of desorption. If ΔN atoms per unit area desorb in time τ , the approximate number of collisions per atom among them in subsequent time t (the TOF to the detector) is $\nu = \sigma \Delta N \times \ln(t/\tau)$, where σ is the collision cross section.⁹ In Taborek's experiments, ν is of order 1 ($\sigma \Delta N \approx 1$ per monolayer desorbed, and the logarithmic factor is always ~ 1). In the present experiments, however, the flux of phonons to the desorbing surface is reduced by more than 3 orders of magnitude because of spreading in the crystal. As a result, ΔN is roughly 10^3 times smaller, and we thus conclude that the collisions are far too few to influence the signal.

Figure 2 shows the TOF measurements at 0° as a function of film thickness. At very low coverage (less than 1 monolayer) the phonoatomic peak is the principal feature, but as the film thickness increases, a thermal peak at longer times starts to develop. Finally, at roughly two monolayers, we approach the results obtained previously by Sinvani and co-workers,^{1,3} i.e.,

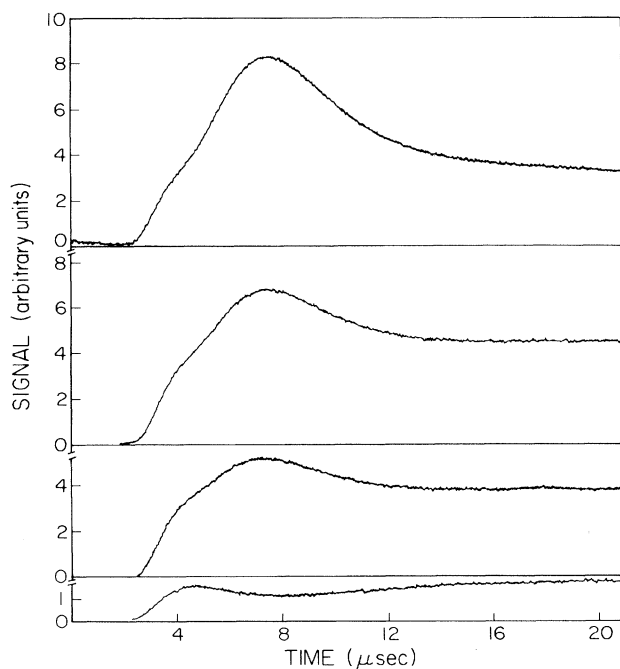


FIG. 2. Time-of-flight spectra at 0° angle for four different coverages with estimated chemical potentials of $\mu \approx -70$ K, -55 K, -40 K, and -30 K, reading from bottom to top.

the thermal peak dominates the signal. In other words, we observe that, on the time scale of our heat pulses, photoatomic desorption dominates in thin films, but thermal processes become more important in thicker films. We return to this issue below.

To be able to study the behavior of these two processes semiquantitatively as a function of chemical potential and angle, we have used a rough deconvolution technique which is basically a four-parameter fit to the signal. The parameters are the magnitudes (S_m) and positions (t_m) of the maxima of the phonoatomic and thermal distributions. Based on the analyses of Sinvani *et al.*,³ the signals are given by

$$S(t) = S_m \frac{t_m^n}{t^n} \frac{|\mu| + ml^2/2t^2}{|\mu| + ml^2/2t_m^2} \times \exp \left[-\beta_{f,n} \frac{m}{2} l^2 \left(\frac{1}{t^2} - \frac{1}{t_m^2} \right) \right],$$

where l is the distance between the desorbing surface and bolometer planes, and

$$\beta_{f,n} \approx \frac{2t_m^2}{ml^2} \left[\frac{n}{2} + \frac{1}{1 + (2|\mu|/ml^2)t_m^2} \right],$$

and where $n=5$ for point source and point detector, and $n=3$ for infinite source and point detector. The phonoatomic and thermal peak temperatures are then given, respectively, by $\beta_{h,n}$ and $\beta_{f,n}$ with $\beta = (k_B T)^{-1}$.

With this technique, the 0° signal can be deconvolved by trial and error. However, as a result of the experimental geometry at 45° , the resolution of the signal's two components is reduced to the extent that the deconvolution leads to ambiguous results. The data in Fig. 1 seem to show only a thermal desorption signal at 45° and were at first thought to be evidence of focusing, but an attempted deconvolution showed some phonoatomic contribution at this angle. Because of the importance of this point, it became evident that the background had to be removed. A new mask was designed, a schematic diagram of which is presented in the inset of Fig. 3. It almost completely removed the background as the signal in Fig. 3 indicates.

Figure 4 shows a typical signal at 0° and 45° , but on a more expanded time scale. As can be seen, a phonoatomic peak is present at 45° . It arrives later than the same peak at 0° by a factor of $\sqrt{2}$, attributable to geometry. There is no rainbow effect, and its magnitude is consistent with a $\cos\theta$ distribution in the desorbed flux. All of our data have these features. Thus, we find neither kinematic focusing due to phonoatomic desorption, nor focusing due to collisions.

The absence of kinematic focusing can be attributed to surface roughness, surface defects, a damaged layer, impurities, or any other mechanism that can lift the assumption of parallel momentum conservation built

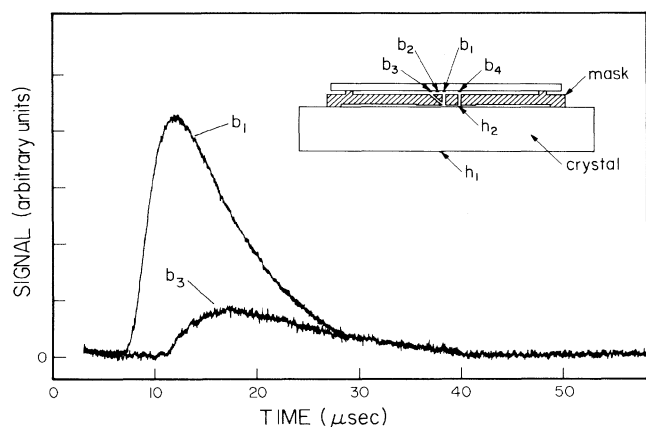


FIG. 3. The new mask, in the inset, and a typical signal at 0° and 45° are shown (from bolometers b_1 and b_3 , respectively). The mask, made of stainless steel, covers the whole desorption surface. The two holes are 1 mm in diameter, one at 45° to the other. The bolometers were 3 mm away from the surface. To enhance the signal size, a typical pulse width used was $1 \mu\text{sec}$. b_2 was used as a heater to match the calibrations of b_1 and b_3 . The heater h_2 and bolometer b_4 were used to measure the chemical potential (Ref. 10) (i.e., film thickness).

into the model. Aside from using optically polished crystals and handling them with standard laboratory care, we, at this stage, have no other means to assess the cleanliness of these surfaces or to improve upon them *in situ*. Several methods to achieve better surfaces are under investigation.

We have also studied the evolution of the phonoatomic effect and thermal desorption as a function of film thickness using the new mask. The same general feature was observed; i.e., it appears that in thin films, the phonoatomic-effect contribution dominates, but as the film thickness increases, desorption becomes mainly thermal.

The thermal component can be understood in terms of the thermal time constant τ of the film, the time it takes for the film to reach steady state. Based on either kinetic theory¹¹ or quantum mechanical calculations,¹² this rate has an exponential behavior: $\tau = \tau_0 \exp(E/k_B T_f)$, where T_f is the film temperature and τ_0 and E are parameters with time and energy units, respectively. E has been shown experimentally to be strongly correlated with the chemical potential.¹³

With the assumption that γ_0 is relatively insensitive to film thickness, the time constant varies by roughly three orders of magnitude from $\mu_1 = -70 \text{ K}$ (our thinnest film) to $\mu_2 = -30 \text{ K}$ (our thickest film), with T_f taken as 4 K, slightly above the ambient temperature, according to the temperature of the thermal component of the signal.

For thick films, it is found that τ is of the order of microseconds, leading to a thin-film time constant of

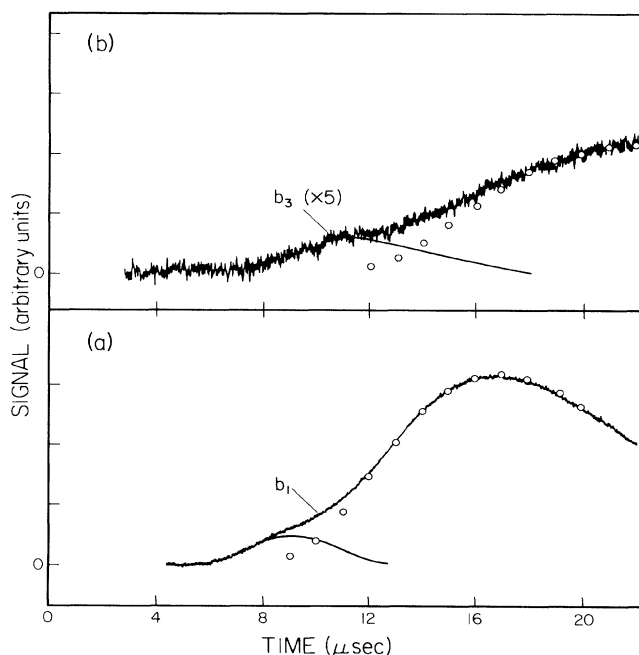


FIG. 4. A typical signal at (a) 0° and (b) 45° is shown on a more expanded time scale than the signal in Fig. 3. The deconvolution technique is depicted, with $n = 5$. The circles represent a fit to the thermal component of the signal, and the solid curve is the subtracted signal (i.e., phonoatomic contribution). $\mu \sim -25 \text{ K}$.

roughly milliseconds. The pulse widths used in these experiments are of the order of $1 \mu\text{sec}$ during which very little thermal desorption can therefore occur in the case of thin films, causing the spectrum to be dominated by the phonoatomic process. But as the film thickness increases, even though the phonoatomic contribution also increases, the thermal desorption rapidly takes over.

There is abundant evidence that desorption of He is a manifestation of the anomalous Kapitza resistance.^{5,14} However, there is no evidence as to whether the mechanism of the phonoatomic effect is related to the Kapitza anomaly since previous experiments concerned with the Kapitza effect could not have detected the contribution of phonoatomic desorption.¹⁵

Another observation was that the temperature assigned to the phonoatomic-effect peak was at most 9 K, whereas the heater temperature was calculated to be 19 K on the basis of the acoustic mismatch model. Apparently, impurity scattering in sapphire (which goes as the fourth power of frequency) and an imperfect interface between heater and crystal both have the effect of allowing only lower-frequency phonons to arrive ballistically at the desorbing surface. These effects have been commonly observed by other investigators.¹⁶

In summary, we have shown that it is possible, by

taking advantage of thermal desorption kinetics, to suppress thermal desorption leaving the phonoatomic effect the principal component of the desorption signal. We have also shown that once all experimental artifacts are carefully eliminated, phonoatomic desorption is not focused normal to the surface, but is influenced by the surface condition. These results stand in striking contrast to previous experimental pictures and provide the basis for further investigation of quantum desorption.

We would like to thank Milton Cole, Michael Weimer, and Robert Housley for useful discussions, Edward Boud for his technical assistance, and Roman Movshovich for his help in preparing our bolometers. This work was supported in part by the Office of Naval Research, under Contract No. N0014-80-C-0447.

(a)Present address: Dipartimento Tecnologie Intersectoriali di Base, Energia Nucleare e delle Energie Alternative, I-00044 Frascati, Italy.

(b)Also at Solid State Physics Department, Soreq Nuclear Research Center, Yavne 70600, Israel, and Physics Department, Technion, Technion City, 32000 Haifa, Israel.

(c)Present address: 201 Physics Building, Syracuse University, Syracuse, N. Y. 13210.

¹M. Sinvani, P. Taborek, and D. Goodstein, *Phys. Lett.* **95A**, 59 (1983).

²S. Balibar, *Phys. Lett.* **51A**, 455 (1975); S. Balibar, J. Buechner, B. Castaing, C. Laroche, and A. Libchabor, *Phys. Rev. B* **18**, 3096 (1978); M. J. Baird, F. R. Hope, and

A. F. G. Wyatt, *Nature (London)* **304**, 325 (1983).

³M. Sinvani, D. L. Goodstein, M. W. Cole, and P. Taborek, *Phys. Rev. B* **30**, 1231 (1984).

⁴F. R. Hope, M. J. Baird, and A. F. G. Wyatt, *Phys. Rev. Lett.* **52**, 1528 (1984).

⁵M. Weimer and D. Goodstein, *Phys. Rev. Lett.* **50**, 193 (1983).

⁶S. C. Ying and B. Bendow, *Phys. Rev. B* **7**, 637 (1973); Z. W. Gortel, H. J. Kreuzer, and S. Spaner, *J. Chem. Phys.* **72**, 234 (1980).

⁷P. Taborek, *Phys. Rev. Lett.* **48**, 1737 (1982).

⁸James P. Cowin, *Phys. Rev. Lett.* **54**, 368 (1985); P. Taborek, private communication.

⁹J. P. Cowin, D. J. Auerbach, C. Becker, and L. Wharton, *Surf. Sci.* **78**, 545 (1978).

¹⁰M. Sinvani and D. Goodstein, *Surf. Sci.* **125**, 291 (1983).

¹¹J. Frenkel, *Kinetic Theory of Liquids* (Dover, New York, 1955).

¹²F. O. Goodman and I. Romero, *J. Chem. Phys.* **69**, 1086 (1978); Z. W. Gortel, H. J. Kreuzer, and R. Teshima, *Phys. Rev. B* **22**, 5655 (1980).

¹³M. Sinvani, P. Taborek, and D. Goodstein, *Phys. Rev. Lett.* **48**, 1259 (1982).

¹⁴R. C. Johnson, and W. A. Little, *Phys. Rev.* **130**, 596 (1963); G. A. Toombs and L. J. Challis, *J. Phys. C* **4**, 1085 (1971); A. R. Long, R. A. Sherlock, and A. F. G. Wyatt, *J. Low Temp. Phys.* **17**, 7 (1974).

¹⁵W. Dietsche and H. Kinder, *J. Low Temp. Phys.* **23**, 27 (1975); C. J. Guo, and H. J. Maris, *Phys. Rev. A* **10**, 960 (1974).

¹⁶A. C. Anderson, in *Nonequilibrium Superconductivity, Phonons and Kapitza Boundaries*, edited by K. E. Gray (Plenum, New York, 1980), and references therein.